Jerzy GOŁĘBIOWSKI, Marek ZARĘBA

Bialystok Technical University, Faculty of Electrical Engineering, Department of Theoretical Electrotechnics and Metrology

doi:10.15199/48.2015.10.57

Plano-parallel models of the electrical systems with non-uniform heat exchange on a perimeter Part II. Transient temperature field

Abstract. *In the article a spatial-temporal heating curve and distribution of the local time constant of the plano-parallel system were determined by the method of states superposition. The heat exchange is characterized by three different coefficients of the heat transfer on a perimeter of the system cross-section. The transient component of the thermal field was found solving the boundary-initial problem for the equation of heat conduction by the separation of variables method. The presented solution can be a mathematical model of the transient thermal field in a rectangular DC busway or in a long dielectric capacitative heated. It was proved that the busway can be approximated by the element of lumped parameters. In opposition to that, long dielectric have to be modeled by the element of distributed parameters. The results were verified by the method of finite elements (program NISA v. 16) and presented in a graphic form.*

Streszczenie. *Za pomocą metody superpozycji stanów w artykule wyznaczono przestrzenno-czasową krzywą rozgrzewu i rozkład lokalnej stałej czasowej układu płasko-równoległego. Wymianę ciepła charakteryzują trzy różne współczynniki jego przejmowania na obwodzie przekroju układu. Składową przejściową pola termicznego uzyskano rozwiązując metodą separacji zmiennych zagadnienie brzegowo-początkowe dla równania przewodnictwa cieplnego. Prezentowane rozwiązanie może stanowić model matematyczny nieustalonego pola termicznego w prostokątnym szynoprzewodzie DC lub w długim dielektryku nagrzewanym pojemnościowo. Wykazano, że szynoprzewód może być aproksymowany elementem o parametrach skupionych. W przeciwieństwie do tego, długi dielektryk musi być modelowany elementem o parametrach rozłożonych. Wyniki sprawdzono za pomocą metody elementów skończonych (program NISA v. 16) i przedstawiono w postaci graficznej.(**Płasko-równoległe modele układów elektrycznych z nierównomiernym oddawaniem ciepła na obwodzie. Część II. Nieustalone pole temperatury**).*

Keywords: analytical methods of the field theory, transient heat flow, heating curves, thermal time constants
Słowa kluczowe: analityczne metody teorii pola, nieustalony przepływ ciepła, krzywe rozgrzewu, termiczne stałe czasowe

Introduction

The second part of the paper is focused on dynamic states of the temperature in plano-parallel systems presented in [13]. The aim of article is determination of parameters of the transient state: spatial-temporal heating curves (step characteristics) and thermal time constants. The mentioned parameters are very important in the analysis of transient states arised in a busway in effect of the supply switching on, the change of a load or a shortage. A knowledge of the mentioned parameters is also useful in the investigation of the possible system overloading by a current larger than the steady state current rating in the process of irregular or interceptive regime [1], [2]. In turn, in case of the capacitative heating, the transient state plays significant role in the rapid heating by a large power [3], [4].

Analogical as in part I of the paper [13], the nonstationary thermal field will be determined by the analytical way.

Mathematical model of the transient component of a heating curve

The heating curve of a model was determined by the method of the states superposition [5], [6]

$$T(x,y,t) = T_o + v_s(x,y) + v_t(x,y,t)\,, \tag{1}$$

where: $v_s(x,y)$, - increase of a temperature of the steady component, $v_t(x,y,t)$ - increase of a temperature of the transient component $(\lim_{t\to\infty} v_t(x,y,t) = 0)$ after the step switching on of heat sources [13, formula (2a,b)], T_o - ambient temperature.

The stationary distribution $v_s(x,y)$ was determined in [13]. For that reason only the transient component of a curve $v_t(x,y,t)$ was analyzed in the present paper.

An initial-boundary problem for the transient component $v_t(x,y,t)$ was formulated on the basis of (1) and taking advantage of a boundary problem of the stationary component $v_s(x,y)$ [13, formulas (2), (3)].

In accordance with the method of states superposition [5], [6], the nonstationary increase $v_t(x,y,t)$ does not depend on an excitation and it is described by the following homogeneous equation

$$\frac{\partial^2 v_t(x,y,t)}{\partial x^2} + \frac{\partial^2 v_t(x,y,t)}{\partial y^2} - \frac{1}{\chi}\frac{\partial v_t(x,y,t)}{\partial t} = 0 \tag{2}$$

for $|x| \le a$ and $0 \le y \le b$, $t > 0$ where:

$\chi=\lambda/(c\delta)$ - diffusivity, λ - specific thermal conductivity δ - density, c - specific heat of a material, t - time, $(2a,b)$ - dimensions of the system cross-section [13, Fig. 1].

Boundary conditions for $v_t(x,y,t)$ are analogical with [13, formulas (3)]

$$\left.\frac{\partial v_t(x,y,t)}{\partial x}\right|_{x=a} = -\frac{\alpha_V}{\lambda} v_t(x=a,y,t)\,, \tag{3a}$$

$$\left.\frac{\partial v_t(x,y,t)}{\partial x}\right|_{x=0} = 0\,, \tag{3b}$$

$$\left.\frac{\partial v_t(x,y,t)}{\partial y}\right|_{y=0} = \frac{\alpha_L}{\lambda} v_t(x,y=0,t)\,, \tag{3c}$$

$$\left.\frac{\partial v_t(x,y,t)}{\partial y}\right|_{y=b} = -\frac{\alpha_H}{\lambda} v_t(x,y=b,t)\,, \tag{3d}$$

where $\alpha_H \neq \alpha_L \neq \alpha_V$ are the heat transfer coefficients on a perimeter of the cross-section shown in [13, Fig. 1]. Then in accordance with the method of states superposition [5], [6], the initial condition of the transient component is equal to the negative stationary component

$$v_t(x,y,t=0) = -v_s(x,y)\,. \tag{4}$$

Relations (2)-(4) formulate the problem of the transient component of a heating curve.

Solution of the boundary-initial problem and determination of heating curves model

The homogeneous equation of heat conduction (2) was solved by the separation of variables [5], [7]. As separation constants $(\gamma_n/b)^2$ and $(\beta_m/a)^2$ were assumed. Advantage of the thermal conditions symmetry with respect to the plane $x=0$ was taken. In the result it was obtained

(5)
$$v_t(x,y,t)=\sum_{m=1}^{\infty}\sum_{n=1}^{\infty}\cos(\beta_m\frac{x}{a})\left[F_{mn}\sin(\gamma_n\frac{y}{b})+G_{mn}\cos(\gamma_n\frac{y}{b})\right]e^{-\chi\left(\frac{\beta_m^2}{a^2}+\frac{\gamma_n^2}{b^2}\right)t}$$

for $|x|\le a$, $0\le y\le b$ and $t>0$, where: F_{mn}, G_{mn} - coefficients of the trigonometric series, β_m,γ_n - dimensionless eigenvalues of the problem. Relation (5) fulfills condition (3b). Then (5) was introduced to (3c). It leads to elimination of the coefficient F_{mn}. Hence it follows, that

(6)
$$v_t(x,y,t)=\sum_{m=1}^{\infty}\sum_{n=1}^{\infty}G_{mn}\cos(\beta_m\frac{x}{a})\left[\frac{\alpha_L b}{\gamma_n\lambda}\sin(\gamma_n\frac{y}{b})+\cos(\gamma_n\frac{y}{b})\right]e^{-\chi\left(\frac{\beta_m^2}{a^2}+\frac{\gamma_n^2}{b^2}\right)t}$$

for $|x|\le a$, $0\le y\le b$ and $t>0$.

Introducing (6) to (3a) the first equation of eigenvalues was obtained as

(7)
$$tg\beta_m=\frac{\alpha_V a}{\beta_m\lambda},$$

where β_m are the consecutive positive roots of (7). In turn, after introduction of (6) to (3d) the second equation of eigenvalues was obtained with respect to the roots γ_n. It is identical as in part I of the paper [13, formula (6)]. For this reason the same constant $(\gamma_n/b)^2$ can be assumed with separation of variables in equations (2) and [13, formula (2)].

The unknown coefficient G_{mn} in (6) should be determined, as well. For this reason an initial condition (4) for the transient component was utilized. After substitution of (6) to (4) and taking advantage of [13, formula (5a)] it was obtained

(8)
$$\sum_{m=1}^{\infty}\sum_{n=1}^{\infty}G_{mn}\cos(\beta_m\frac{x}{a})\left[\frac{\alpha_L b}{\gamma_n\lambda}\sin(\gamma_n\frac{y}{b})+\cos(\gamma_n\frac{y}{b})\right]=-v_s(x,y)=$$
$$=-\left(-\frac{gy^2}{2\lambda}+B\frac{\alpha_L}{\lambda}y+B\right)-\sum_{k=1}^{\infty}D_k\cosh(\gamma_k\frac{x}{b})\left[\frac{\alpha_L b}{\gamma_k\lambda}\sin(\gamma_k\frac{y}{b})+\cos(\gamma_k\frac{y}{b})\right],$$

where: B, D_k were determined in [13, formulas (5b) and (9)] and the indices were changed $n\to k$ in the last component of the right side of (8).

Then relation (8) was multiplied by $\cos(\beta_i x/a)$ and integrated by sides in a sector $\langle -a,a\rangle$ with respect to the coordinate x. Analogical operations were done with the aid of function $\left(\frac{\alpha_L b}{\gamma_l\lambda}\sin(\gamma_l\frac{y}{b})+\cos(\gamma_l\frac{y}{b})\right)$ in a sector $\langle 0,b\rangle$ with respect to the coordinate y. Advantage was taken of the sequence $\left(\frac{\alpha_L b}{\gamma_l\lambda}\sin(\gamma_l\frac{y}{b})+\cos(\gamma_l\frac{y}{b})\right)$ orthogonality in a sector $\langle 0,b\rangle$ (proved in [13, appendix]) and of the sequence $\cos(\beta_i x/a)$ in a sector $\langle -a,a\rangle$ (proof is given in an appendix to the present article). Finally, the coefficient G_{il} is expressed below

(9)
$$G_{il}=\frac{-\int_0^b\int_{-a}^{a}v_s(x,y)\left(\cos(\beta_i\frac{x}{a})\right)\left(\frac{\alpha_L b}{\gamma_l\lambda}\sin(\gamma_l\frac{y}{b})+\cos(\gamma_l\frac{y}{b})\right)dxdy}{\|I(i)\|^2\cdot\|I(l)\|^2},$$

where:

$\|I(l)\|^2=\int_0^b\left(\frac{\alpha_L b}{\gamma_l\lambda}\sin(\gamma_l\frac{y}{b})+\cos(\gamma_l\frac{y}{b})\right)^2dy$ - is a square of the norm [8] of the sequence $\left(\frac{\alpha_L b}{\gamma_l\lambda}\sin(\gamma_l\frac{y}{b})+\cos(\gamma_l\frac{y}{b})\right)$,

$\|I(i)\|^2=\int_{-a}^{a}\cos^2(\beta_i\frac{x}{a})dx$ - square of a norm of the sequence $\cos(\beta_i\frac{x}{a})$.

It is worth to notice, that $v_s(x,y)$ introduces to (9) a third index k (next to i, l). It follows from the right side of (8). Hence with the computation of integrals in (9) orthogonality of the functional sequences with arguments $(\gamma_k y/b)$ and $(\gamma_l y/b)$ should be considered in a sector $\langle 0,b\rangle$. It leads to a closed form of G_{il}. After taking advantage of eigenvalues equations and some simplifications it was obtained

(10)
$$G_{il}=\frac{-2gab^3\sin(\beta_i)\left[\alpha_H\sin(\gamma_l)\left(b^2\alpha_L^2+\gamma_l^2\lambda^2\right)+\lambda\gamma_l b\alpha_L(\alpha_L+\alpha_H)\right]}{\|I(i)\|^2\cdot\|I(l)\|^2\lambda^3(\alpha_L+\alpha_H)\beta_i\gamma_l^5}-$$
$$-D_l\frac{2ab\left[b\beta_i\cosh\left(\gamma_l\frac{a}{b}\right)\sin(\beta_i)+a\gamma_l\sinh\left(\gamma_l\frac{a}{b}\right)\cos(\beta_i)\right]}{\left(b^2\beta_i^2+a^2\gamma_l^2\right)\|I(i)\|^2},$$

where:

(11)
$$\|I(i)\|^2=a\left(1+\frac{\alpha_V a}{\beta_i^2\lambda}\cos^2\beta_i\right),$$

(12)
$$\|I(l)\|^2=\frac{\left(\lambda^2\gamma_l^2+b^2\alpha_L^2\right)\left[\sin^2(\gamma_l)\left(\alpha_L\alpha_H b^2+\lambda^2\gamma_l^2\right)+\lambda\gamma_l^2 b(\alpha_L+\alpha_H)\right]}{2\lambda^3\gamma_l^4(\alpha_L+\alpha_H)}.$$

Finally, after superposition with respect to relation (1) the spatial-temporal curves $T(x,y,t)$ of heating were obtained. The second component of (1) was determined in [13, formula (5a)], and the third one is described by (6) (where G_{mn} results from (10)-(12) after the exchange $i\to m$, $l\to n$).

Thermal time constants

After consideration of determined distributions $v_s(x,y)$ and $v_t(x,y)$ in (1), it is hard to evaluate duration of the transient state on the basis of $T(x,y,t)$. For this reason it is determined with some approximation with the aid of the known criterion of an averaged (locally) time constant [14], [15]. It relies on approximation of each point of the system by the first order inert element. The step response of such an object is generally known, as

(13)
$$T(x,y,t)=T_s(x,y)\left(1-e^{-\frac{t}{\tau(x,y)}}\right)+T(x,y,t=0)e^{-\frac{t}{\tau(x,y)}},$$

where $\tau(x,y)$ - averaged (locally) time constant.

After determination of $e^{-\frac{t}{\tau(x,y)}}$ from equation (13) and integration by sides with respect to a time t one obtains $\tau(x,y)$ in the form [9], [10], [11]

$$\tau(x,y)=\int_0^{\infty}\frac{T(x,y,t)-T_s(x,y)}{T(x,y,t=0)-T_s(x,y)}dt=\int_0^{\infty}\frac{v_t(x,y,t)}{v_t(x,y,t=0)}dt \quad (14)$$

where (1) was utilized. Introduction of (6) to (14) leads to determination of the investigated time constant

(15)

$$\tau(x,y)=\frac{\sum_{m=1}^{\infty}\sum_{n=1}^{\infty}G_{mn}\frac{a^2b^2}{\chi(\beta_m^2b^2+\gamma_n^2a^2)}\cos(\beta_m\frac{x}{a})\left[\frac{\alpha_L b}{\gamma_n\lambda}\sin(\gamma_n\frac{y}{b})+\cos(\gamma_n\frac{y}{b})\right]}{\sum_{m=1}^{\infty}\sum_{n=1}^{\infty}G_{mn}\cos(\beta_m\frac{x}{a})\left[\frac{\alpha_L b}{\gamma_n\lambda}\sin(\gamma_n\frac{y}{b})+\cos(\gamma_n\frac{y}{b})\right]}.$$

Distributed parameters of the analyzed system cause, that heating curves at each of its point grow with a different time constant. Duration of the transient state at a location (x,y) is estimated for $4\tau(x,y)$.

Computational examples

The spatial-temporal heating curves and time constants of the investigated systems were determined with the use of Mathematica 7.0 package [12]. Data sets from [13, (12), (13)] were supplemented by the following parameters: for a busway $c=910J/(kgK)$, $\delta=2720kg/m^3$ and $\rho(T_{śr}=62.5^oC)=3.545\cdot10^{-8}\Omega m$ and for a fir plank $c=2400J/(kgK)$, $\delta=450kg/m^3$.

Double series in (6) (similarly as the single one in [13]) occurred to be rapid convergent. For a busway the three terms of the expansion of each sum in (6) were considered. Adding ten consecutive terms in both sums causes for $t>5s$ a change of the result just on 8-th position after the decimal point at each point of the system. In turn, in computations of a dielectric charge 50 terms of each sum in (6) were considered. The increase of indices to 100 in the both sums of (6) causes for $t>5s$ a change of the result on 4-th position after the decimal point at the points of the slowest convergence.

The results of computations of both models were shown in a graphic form. In Fig. 1, 2 spatial distributions of the field in a busway were shown for smaller and larger instants, respectively. In turn, in Fig. 3, 4 temperature distributions in the fir plank were illustrated at analogical time instants. In Fig. 5, 6 heating curves were shown at the selected points, in a busway and in a wood, respectively. In Fig. 7 distribution of the averaged (local) time constant in a fir plank was illustrated. For the busway a value of the time constant is ca. $\tau=878.6s$ and practically doesn't change its value in the whole region. For this reason its diagram was not included.

The presented method was verified analogously as in [13]. For this aim the obtained results were compared with computations realized with the aid of the NISA programme [16] by the finite element method [17]. Namely to [13, formula (14)] distributions (1) at the selected time instants were introduced. In the result relative differences in a busway were illustrated in Fig. 8, and in a fir plank in Fig. 9. It was checked, that relative differences for larger times do not exceed 0.0023% at a busway and 0.08% at a fir plank (for $|x|\le a$, $0\le y\le b$).

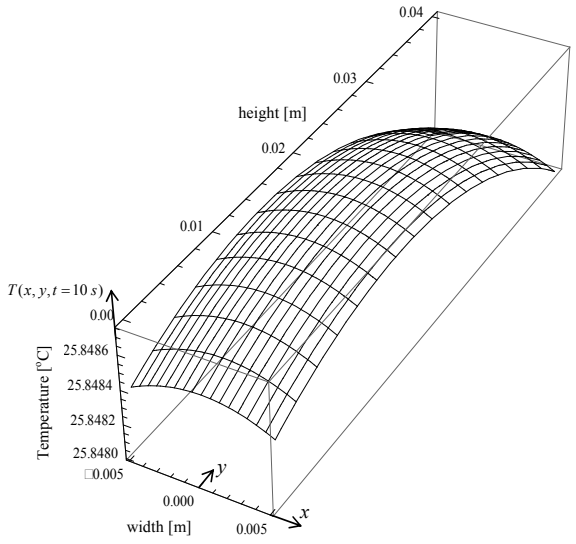

Fig. 1 Spatial distribution of the thermal field in a busway at the instant t=10 s

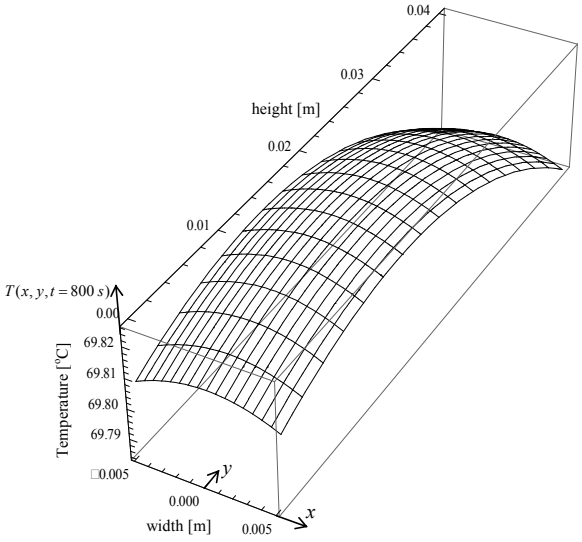

Fig. 2 Spatial distribution of the thermal field in a busway at the instant t=800 s

Final remarks

A) It follows from Fig. 1 and Fig. 2, that for smaller and larger times the spatial temperature distributions in a busway are close to uniform ones. A physical reason of that phenomenon is the large thermal conductivity of aluminum. It can be noticed, as well, that distributions at the consecutive time instants and the stationary one in [13] show a close similarity. However they are significantly shifted with respect to each other along the temperature axis.

In turn, in the capacitative heating analysis (Fig. 3, 4) much more uniformity of the field distribution can be noticed for shorter times (Fig. 3) than for the longer ones (Fig.4). The small thermal conductivity of wood causes, that at the beginning of the transient state the influence of a cooling process of the system on a shape of the field is relatively small. In that time period a dominant role in the forming of distributions play heat sources (which are uniform). The similar effect was noticed in the paper [4], as well, in which one dimensional problem of the food heating was analyzed

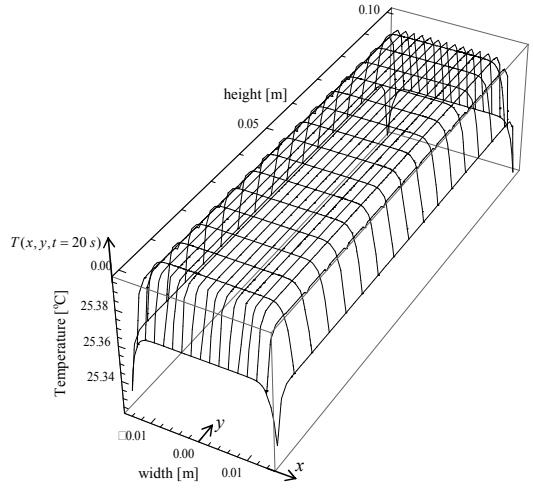

Fig. 3 Spatial distribution of the thermal field in a fir plank at the instant t=20 s

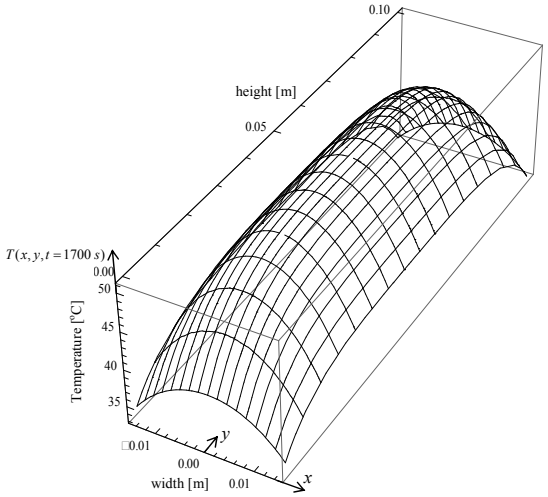

Fig. 4 Spatial distribution of the thermal field in a fir plank at the instant t=1700 s

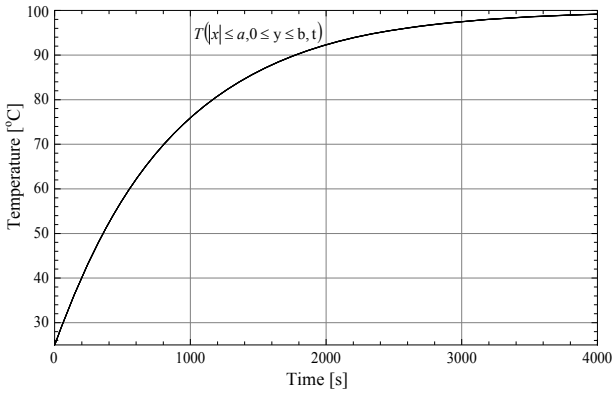

Fig. 5 Heating curve of the busway

B. A large value of the thermal conductivity of a busway causes, that the time constant is practically the same (τ=878.6s) at the whole area {for $|x| \le a$ and $0 \le y \le b$}. It confirms practically the same heating curves (Fig. 5) at different points of the system. Then in the busway a spatial distribution of the field can be neglected and it can be treated as the element with lumped parameters. In turn, in case of capacitative heating the heating curves (Fig.6) and the time constant (Fig. 7) significantly depend on the point location. Larger vales of $\tau(x,y)$ can be observed in Fig. 7 at a half of the height of a fir plank i.e. with $y \approx b/2$ for $|x| \le a$. The same conclusion follows from Fig. 6 (after the consideration, that each curve possess its own asymptote and a tangent). Then the heated dielectric is the element of distributed parameters.

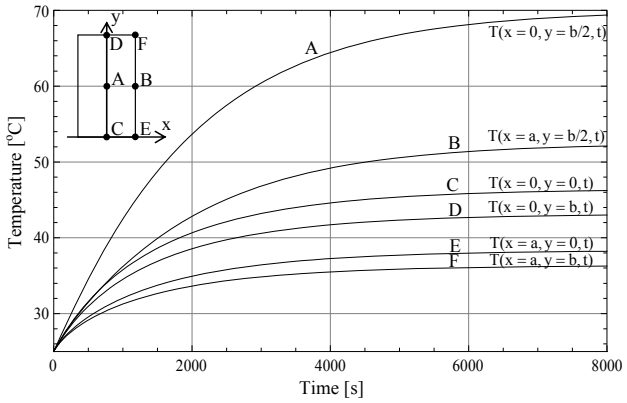

Fig. 6 Heating curves at the selected points of a fir plank

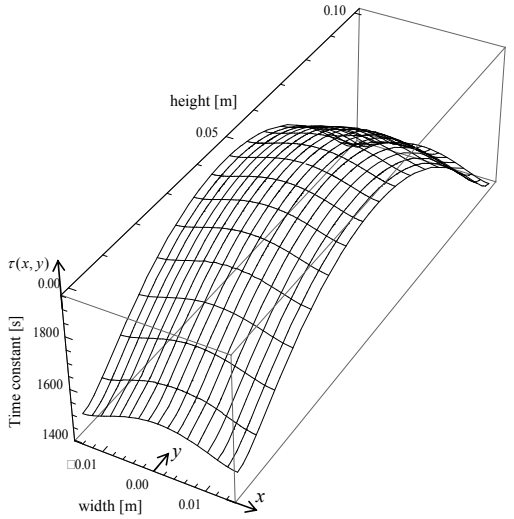

Fig. 7 Averaged time constant in a fir plank in the function of geometrical coordinates

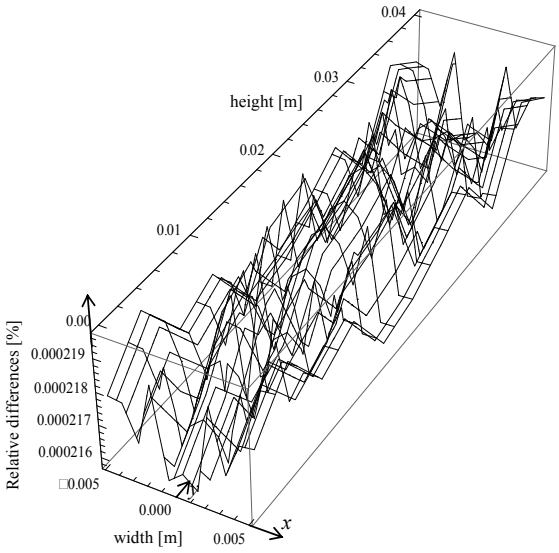

Fig. 8 Relative differences of the temperature distributions obtained in a busway by the finite element method and by the analytical one at the instant t=10 s

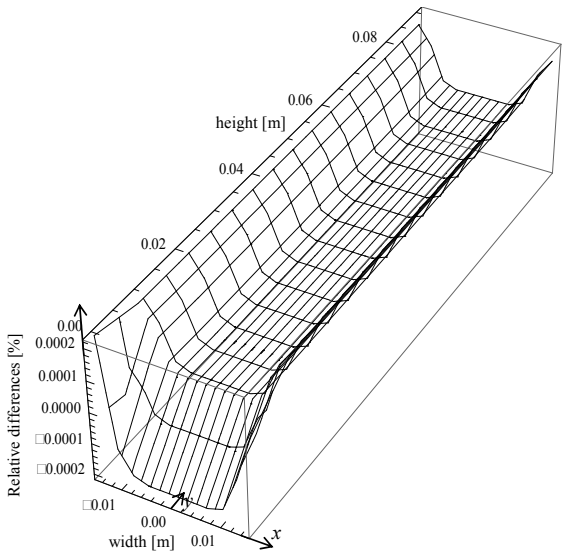

Fig. 9 Relative differences of the temperature distributions obtained in a fir plank by the finite element method and by the analytical one at the instant t=1700 s

C. In the both considered systems (for shorter and longer times) relative differences of the field distributions (computed in the analytical and by the numerical way) are very small. It is illustrated for example in Fig. 8 and in Fig. 9. Therefore the method presented here is verified.

ACKNOWLEDGMENT

The article was prepared in a framework of the project S/WE/1/13 realized in the Chair of Theoretical Electrotechnic and Metrology in the Polytechnic of Bialystok.

Appendix

Proof of an orthogonality of the sequence $\cos(\beta_m \frac{x}{a})$ in a sector $\langle -a, a \rangle$.

For $n \neq m$ it takes place

$$I(n,m) = \int_{-a}^{a} \cos\left(\beta_m \frac{x}{a}\right)\cos\left(\beta_n \frac{x}{a}\right)dx =$$

$$= \frac{2a\beta_m}{\left(\beta_m^2 - \beta_n^2\right)}\cos\beta_n \sin\beta_m - \frac{2a\beta_n}{\left(\beta_m^2 - \beta_n^2\right)}\cos\beta_m \sin\beta_n.$$

Introducing the equation of eigenvalues (7) in the form $\sin\beta_m = \frac{\alpha_V a}{\beta_m \lambda}\cos\beta_m$ and the same relation but with respect to the series β_n to the above formula, in the result one obtains

(16) $$I(n,m) =$$

$$\frac{2a^2\alpha_V}{\lambda\left(\beta_m^2 - \beta_n^2\right)}\cos\beta_n\cos\beta_m - \frac{2a^2\alpha_V}{\lambda\left(\beta_m^2 - \beta_n^2\right)}\cos\beta_n\cos\beta_m = 0.$$

A square of the norm of the considered sequence is equal to

$$\left\|N(n)\right\|^2 = \int_{-a}^{a} \cos^2(\beta_n \frac{x}{a})dx = a\left(1 + \frac{\sin\beta_n\cos\beta_n}{\beta_n}\right).$$

After introduction of the eigenvalues equation and some simplifications it was obtained, that

(17) $$\left\|N(n)\right\|^2 = a\left(1 + \frac{\alpha_V a}{\beta_n^2 \lambda}\cos^2\beta_n\right) > 0.$$

Then finally from relations (16) and (17) follows

$$I(n,m) = \int_{-a}^{a} \cos(\beta_m \frac{x}{a})\cos(\beta_n \frac{x}{a})dx = \begin{cases} 0 & for\ \ n \neq m \\ \left\|N(n)\right\|^2 > 0 & for\ \ n = m \end{cases}$$

QED (quod erat demonstrandum).

REFERENCES

[1] Kulas S., Tory prądowe i układy zestykowe, (Current ducts and contact systems), *Oficyna Wydawnicza Politechniki Warszawskiej*, Warszawa (2008) (in Polish).
[2] Maksymiuk J., Pochanke Z., Obliczenia i badania diagnostyczne aparatury rozdzielczej, (Computation and diagnostic investigations of power distributing apparatus), *WNT*, Warszawa (2001) (in Polish).
[3] Hering M., Podstawy elektrotermii. Część II, (Fundamentals of electric heating engineering. Part II), *WNT*, Warszawa (1998) (in Polish).
[4] Fleischman G. J., Predicting temperature range in food slabs undergoing short- term/high-power microwave heating, *Journal of Food Engineering*, 40 (1998), 81-88.
[5] Kącki E., Równania różniczkowe cząstkowe w zagadnieniach fizyki i techniki, (Partial differential equations in the problems of physics and technology), *WNT*, Warszawa (1992) (in Polish).
[6] Hering M., Termokinetyka dla elektryków, (Thermokinetics for electricians), *WNT*, Warszawa (1980) (in Polish).
[7] Evans L. C., Równania różniczkowe cząstkowe, (Partial differential equations), *PWN*, Warszawa (2002) (in Polish).
[8] Latif M. J., Heat conduction, *Springer-Verlag*, Berlin, Haidelberg (2009).
[9] Brykalski A., Ein Beitrag zur Bestimmung der mittleren Zeitkonstante von Diffusionsprozessen, *International Journal of Heat and Mass Transfer*, 28 (1985), n. 3, 613-620.
[10] Lipiński W., Gołębiowski J., Modeling of electromagnetic shield dynamics, *IEEE Transactions on Magnetics*, 16 (1980), n.6, 1419-1422.
[11] Gołębiowski J., Zaręba M., A method of the analysis of the thermal field dynamics in a core and insulation of a DC lead with convectional heat abstraction, *Electrical Engineering-Archiv für Elektrotechnik* , 88 (2006), n.5, 453-464.
[12] Grzymkowski R., Kapusta A., Kumoszek T., Słota D., Mathematica 6, *Wydawnictwa Pracowni Komputerowej Jacka Skalmierskiego*, Gliwice (2008) (in Polish).
[13] Gołębiowski J., Zaręba M., Plano-parallel models of the electrical systems with non-uniform heat exchange on a perimeter. Part I. Stationary thermal field, *Przegląd Elektrotechniczny*.
[14] Lipiński W., Analysis of the electromagnetic field dynamics in conducting media, *Wydawnictwo Uczelniane Politechniki Szczecińskiej*, Seria: Prace Naukowe nr 63, Szczecin (1976).
[15] Brykalski A., Investigation of the dynamics of electromagnetic and thermal processes in electrical devices by numerical methods of the field analysis, *Wydawnictwo Uczelniane Politechniki Szczecińskiej*, Seria: Prace Naukowe nr 343, Szczecin (1987).
[16] Manuals for NISA v. 16. NISA Suite of FEA Software (CD-ROM), *Cranes Software*, Inc., Troy, MI (2008).
[17] Sikora J., Numeryczne metody rozwiązywania zagadnień brzegowych, (Numerical methods for solving boundary problems), *Politechnika Lubelska*, Lublin (2011).

***Authors**: Prof. J. Gołębiowski[1], M. Zaręba[2], Ph. D., Białystok Technical University, Faculty of Electrical Engineering, Wiejska 45D st.,15-351 Białystok, e-mail: [1] j.golebiowski@pb.edu.pl, [2] m.zareba@pb.edu.pl*